

# **Electrochemical Evidence for Catalytic Water Oxidation Mediated by a High-Valent Cobalt Complex**

Derek J. Wasylenko,<sup>a</sup> Chelladurai Ganesamoorthy,<sup>a</sup> Javier Borau Garcia,<sup>a</sup> Curtis P. Berlinguette<sup>a\*</sup>

**Department of Chemistry and Institute for Sustainable Energy, Environment & Economy,  
University of Calgary, 2500 University Drive N.W., Calgary, Canada T2N-1N4.**

E-mail: [cberling@ucalgary.ca](mailto:cberling@ucalgary.ca)

## Synthesis and Characterization

Preparation of **1**.  $[\text{Co}^{\text{II}}(\text{Py5})(\text{OH}_2)](\text{ClO}_4)_2$  was prepared by stirring **Py5<sup>1</sup>** (0.10 g, 0.21 mmol) and  $\text{Co}(\text{ClO}_4)_2 \cdot 6\text{H}_2\text{O}$  (0.077 g, 0.21 mmol) in a 100-mL round-bottom flask with ~50 mL of MeOH/H<sub>2</sub>O (3:1) under N<sub>2</sub> for 24 h. After the solvent was reduced to ~6 mL, the pale yellowish precipitate was filtered, washed with H<sub>2</sub>O (~3 mL) and left to dry in air. Yield: 0.13 g (81 %). Elemental analysis calculated (%) for C<sub>29</sub>H<sub>27</sub>Cl<sub>2</sub>N<sub>5</sub>O<sub>11</sub>Co: C 46.36, H 3.62, N 9.32; found: C 46.24, H 3.68, N 9.24. HR-ESI-MS: calculated for  $[\text{Co}^{\text{II}}(\text{Py5})(\text{OH}_2)]^{2+}$ : 267.066464 *m/z*; found: 267.066459 *m/z*. Single crystals of **1** suitable for X-ray diffraction were prepared by a slow evaporation of the aqueous solution to form pale yellow blocks.

**Physical Methods.** Electrochemical measurements were recorded using Milli-Q H<sub>2</sub>O ( $R = 18.2 \text{ M}\Omega$ ) with a Princeton Applied Research VersaStat 3 potentiostat, a glassy carbon working electrode (diameter = 3 mm), a Pt wire counter electrode and a [Ag]/[AgCl] reference electrode (sat. KCl, 0.197 V vs NHE). Potentials reported herein are referenced to a normal hydrogen electrode (NHE). The glassy carbon working electrode was polished between runs with an alumina slurry to achieve a mirror finish, then thoroughly rinsed with water and sonicated successively in Milli-Q H<sub>2</sub>O, absolute ethanol, and dichloromethane and left to air dry. Buffers solutions were used to achieve the various pH range; i.e., a NaOAc/HOAc buffer (0.1 M) solution at pH <4, and a phosphate buffer (0.1 M KH<sub>2</sub>PO<sub>4</sub> or 0.1 M K<sub>2</sub>HPO<sub>4</sub>) at higher pH levels. The pH was adjusted by adding aliquots of KOH for the phosphate buffer, or HNO<sub>3</sub> for the acetate buffer.

Note that we sought to independently verify the catalytic behavior observed by cyclic voltammetry by monitoring the rate of dioxygen evolution in the headspace of the reaction flask upon the addition of a terminal oxidant. Unfortunately, a number of practical issues persist in basic media. For example, the commonly used terminal single-electron oxidant,  $(\text{NH}_4)_2[\text{Ce}(\text{NO}_3)_6]$  (CAN), requires a low pH to avoid forming hydrolytic products (see P. Yu and T. J. O'Keefe, *J. Electrochem. Soc.*, 2006, **153**, C80-C85) Note that dissolving CAN at higher pH levels will inevitably lead to a strongly acidic medium (due to hydrolysis) thereby shunting catalysis. Dioxygen formation was observed in experiments with OCl<sup>-</sup> and HSO<sub>5</sub><sup>-</sup> from Oxone®; however, the dioxygen was not derived from water (an issue that is extensively documented with this particular document). While we continue to seek out chemical oxidants capable of generating Co(IV) in basic media, we are unfortunately not yet able to offer any positive results in this regard. Experimental details are as follows: headspace dioxygen evolution was monitored using a custom-built apparatus consisting of a round-bottom flask equipped with a septum and a threaded side

arm for insertion of the probe (working volume = 13.8 mL). The flask was charged with a solution of  $[\text{Co}^{\text{II}}(\text{Py5})(\text{OH}_2)]^{2+}$  in 1.0 mL of 0.1 M HOAc/NaOAc buffer (pH 4.6) for experiments with Oxone®, or 0.1 M HClO<sub>4</sub> for the  $(\text{NH}_4)_2[\text{Ce}(\text{NO}_3)_6]$  (CAN) experiments to achieve a catalyst concentration of ~0.13 mM. The headspace was purged with N<sub>2(g)</sub> for *ca.* 20 min until a stable reading was obtained. The solution was not purged to ensure O<sub>2</sub> saturation of the solution for a rapid exclusion of O<sub>2</sub> into the gas phase. A freshly prepared, deaerated solution containing Oxone® or CAN was then injected through a rubber septum sufficient for 50 turnovers (TONs), and stirred in a temperature-modulated oil bath (30 ± 2 °C) for the duration of the experiment. Dioxygen evolution was monitored every 10 s with an optical probe (Ocean Optics FOXY-OR125-AFMG) and a multifrequency phase fluorimeter (Ocean Optics MFPF-100). Data from the sensor was processed by the TauTheta Host Program and then converted into the appropriate calibrated O<sub>2</sub> sensor readings in “% O<sub>2</sub>” by the OOI Sensors application. Standard deviations of the O<sub>2</sub> readings given by the instrument were determined to be ± 3% of the total moles of O<sub>2</sub> produced from successive control experiments. The <sup>18</sup>OH<sub>2</sub> labeling studies were performed using water containing 9.87% <sup>18</sup>OH<sub>2</sub> on a weight basis that was prepared from a bulk 98.7% <sup>18</sup>OH<sub>2</sub> solution purchased from Cambridge Isotopes Labs. Reactions were performed in the same apparatus as used for the dioxygen evolution studies. In a typical experiment, 1 mL of <sup>18</sup>OH<sub>2</sub> (9.87%) was added to the flask followed by an appropriate amount of concentrated acid solution (glacial acetic acid; 17.4 M). The flask was sealed after addition of **1** to reach a concentration of 13 mM; the solution and headspace were then purged with N<sub>2(g)</sub> until a stable dioxygen reading was obtained (*ca.* 20-30 min). A deaerated solution of Oxone® dissolved in 9.87% <sup>18</sup>OH<sub>2</sub> was then injected via syringe into a stirring solution of **1**. After the dioxygen reading stabilized, a 10-20 μL sample of the headspace was directly injected into a Varian 210GC/MS Ion Trap containing a Molsieve 5Å gas separation column and an ion-trap set to focus on ions within the *m/z* 20-80 range. Traces of individual ions were determined by extracting the desired *m/z* value from the spectrum; relative concentrations of isotopes were determined by integrating the area under the signal of the appropriate extracted *m/z* value. Introduction of atmospheric oxygen inherent to this method was corrected for by repeated injections of pure N<sub>2</sub> and noting the ratio of O<sub>2</sub>/N<sub>2</sub>, which was found to be 1.7 ± 0.4%. This ratio was then subtracted from the <sup>32</sup>O<sub>2</sub> signal in the labeled <sup>18</sup>OH<sub>2</sub> studies.

Aqueous phase oxygen evolution experiments were conducted using the same electrochemical apparatus as described above, except the fluorescence probe was immersed in the solution next to the working electrode. The solution was then thoroughly purged with N<sub>2</sub> until a stable baseline was achieved. Electrolysis was then initiated without stirring at an applied potential of 1.6 V vs NHE and the O<sub>2</sub> level was monitored for 10 minutes. Note that quantification of O<sub>2</sub> is not possible since we are only measuring the O<sub>2</sub> concentration near the electrode surface.

QuickTime™ and a decompressor are needed to see this picture.

**Fig. S1.** ORTEP plot of  $[\text{Co}^{\text{II}}(\text{Py5})(\text{OH}_2)](\text{ClO}_4)_2$ .

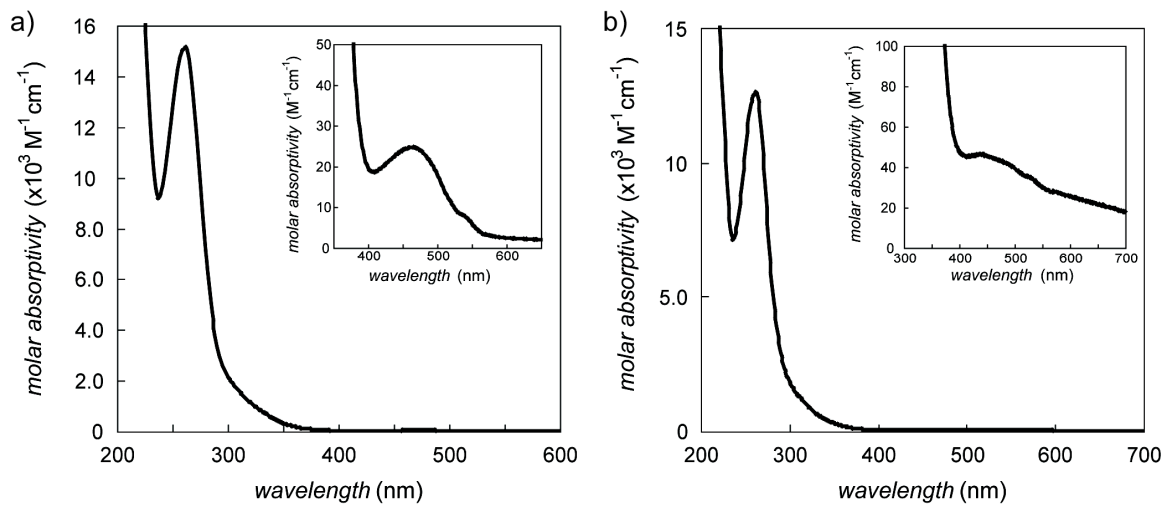


**Fig. S2.** UV-vis spectra of **1** in (a) MeCN (1.07 mM) and (b) H<sub>2</sub>O (0.133 mM).

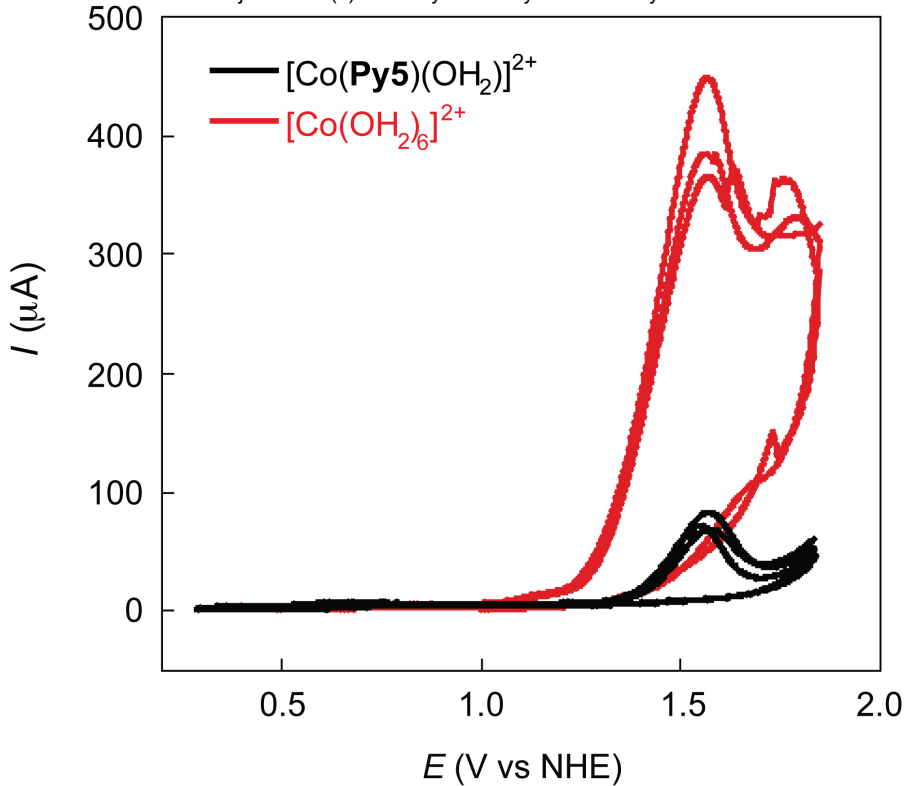


**Fig S3.** Cyclic voltammogram of 1 mM solutions of  $[\text{Co}(\text{OH}_2)_6](\text{ClO}_4)_2$  (red) and  $[\text{Co}(\text{Py5})(\text{OH}_2)](\text{ClO}_4)_2$  (black) in 0.1 M KPi (pH 9) at a scan rate of  $10 \text{ mV s}^{-1}$ . The  $E_{\text{p,a}}$  values of the first anodic peaks are offset (*e.g.*,  $E_{\text{p,a}} [\text{Co}(\text{OH}_2)_6]^{2+} = +1.52 \text{ V}$ ;  $E_{\text{p,a}} [\text{Co}(\text{OH}_2)_6]^{2+} = +1.58 \text{ V}$ ), and there are no additional features appearing in the cyclic voltammograms of  $[\text{Co}(\text{Py5})(\text{OH}_2)]^{2+}$  at a variety of scan rates and the current of the Co(III)/Co(II) redox couple remains static after each cycle, thus indicating that the formation of other species from catalyst degradation is not occurring. It should also be noted that are no other features apparent in the cyclic voltammogram of the  $[\text{Co}(\text{OH}_2)_6]^{2+}$  solution below  $+1.0 \text{ V}$ . Although the apparent similarities in  $E_{\text{p,a}}$  are noted, but are ascribed to the coincident electrochemical potentials of the the deposited Co-oxide film and the  $[\text{Co}^{\text{IV}}(\text{Py5})(\text{OH})]^{3+}/[\text{Co}^{\text{III}}(\text{Py5})(\text{OH})]^{2+}$  redox wave. The noisy electrochemical response of  $[\text{Co}(\text{OH}_2)_6]^{2+}$  (red) is a result of bubbles visibly forming on the electrode surface.

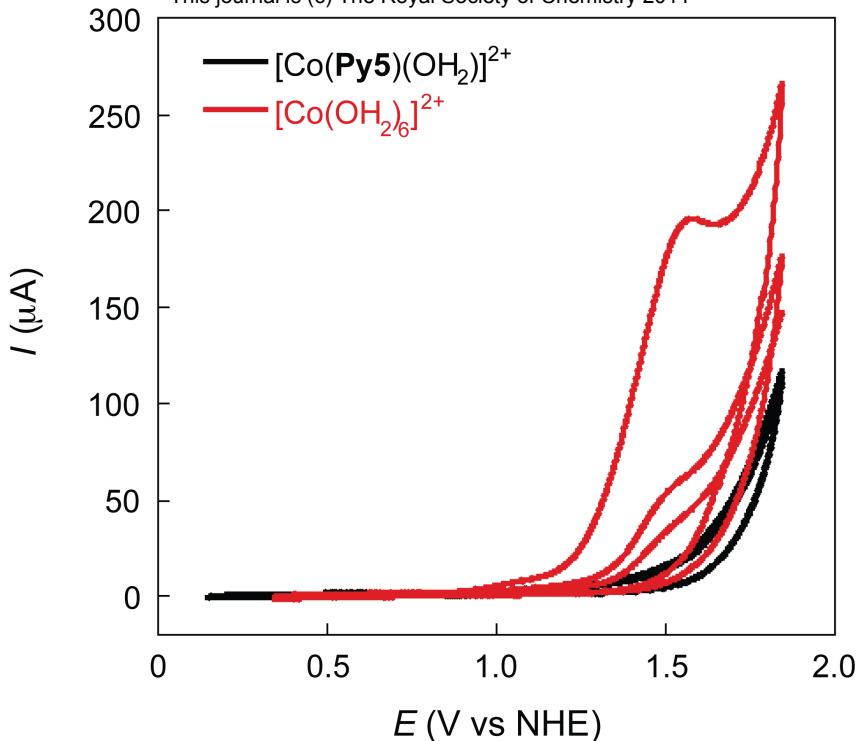


**Fig. S4.** Homogeneity test of electrode surface. This figure depicts the cyclic voltammetric response (scan rate = 10 mV s<sup>-1</sup>) of the glassy carbon working electrode (diameter = 3 mm) in a blank electrolyte (0.1 M KP<sub>i</sub>) following two anodic cycles from 0 - 1.8 V vs NHE (ending at 1.8 V; scan rate = 10 mV s<sup>-1</sup>) in 1 mM solutions of  $[\text{Co}(\text{OH}_2)_6](\text{ClO}_4)_2$  (red) or  $[\text{Co}(\text{Py5})(\text{OH}_2)](\text{ClO}_4)_2$  (black). The electrode was taken out of the solution, thoroughly rinsed with distilled, deionized water and left to air-dry prior to further testing. After anodic cycling in the  $[\text{Co}(\text{OH}_2)_6]^{2+}$  solution, a blue film is visible on the electrode surface; this same film is not visible after anodic cycling of the  $[\text{Co}(\text{Py5})(\text{OH}_2)]^{2+}$  solution. Taken together with the lack of any significant features in the cyclic voltammogram of the electrode after anodic cycling in a  $[\text{Co}(\text{Py5})(\text{OH}_2)]^{2+}$  solution (black line) suggests that the formation of the Co-oxide film is not promoted on the electrode surface following anodic cycling in the  $[\text{Co}(\text{Py5})(\text{OH}_2)]^{2+}$  solution; *i.e.*, the electrochemical response observed in the cyclic voltammogram in Fig. 3 is a result of the  $[\text{Co}(\text{Py5})(\text{OH}_2)]^{2+}$  complex rather than the formation of a heterogeneous film.

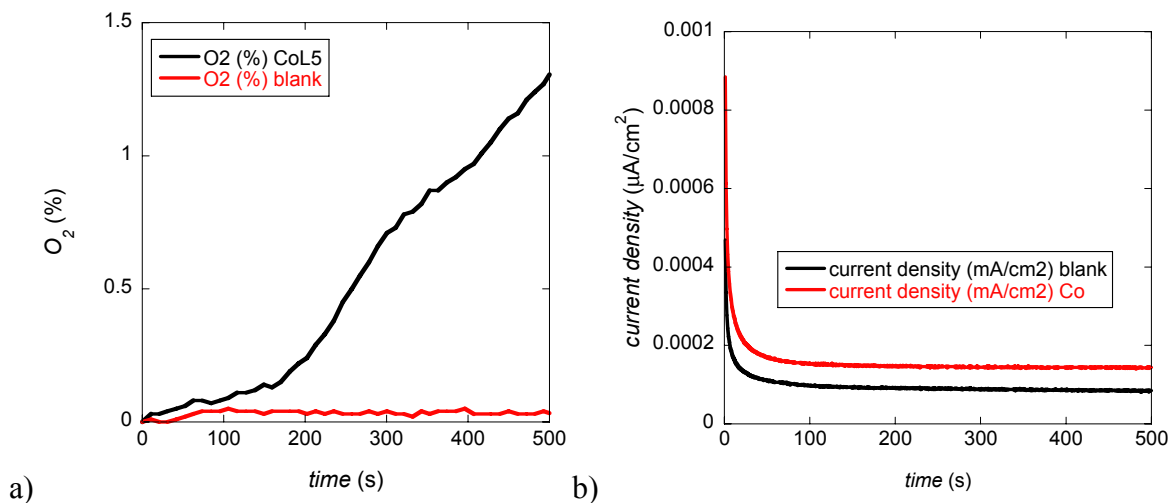


**Fig. S5.** (a) Dioxygen evolution measured by a fluorescence optical probe immersed in the catalytic reaction solution near the working electrode. (b) Time-dependent current density plot recorded concurrently with dioxygen evolution in (a) showing no evidence of catalyst decomposition over 500 s.

QuickTime™ and a  
decompressor  
are needed to see this picture.

**Fig. S6.** Select molecular orbitals of the  $[\text{Co}^{\text{III}}\text{-OH}]^{2+}$  form of **1** calculated by DFT theory.

QuickTime™ and a  
decompressor  
are needed to see this picture.

**Fig. S7.** Select molecular orbitals of the  $[\text{Co}^{\text{IV}}\text{-OH}]^{3+}$  form of **1** calculated by DFT theory.

**Table S1.** Crystal data and structure refinement for **1**

Identification code	[Co( <b>Py5</b> )(OH <sub>2</sub> )](ClO <sub>4</sub> ) <sub>2</sub> , ( <b>1</b> )(ClO <sub>4</sub> ) <sub>2</sub> .	
Empirical formula	C <sub>29</sub> H <sub>27</sub> Cl <sub>2</sub> CoN <sub>5</sub> O <sub>11</sub>	
Formula weight	751.39	
Temperature	173(2) K	
Wavelength	0.71073 Å	
Crystal system	Monoclinic	
Space group	P 21/c	
Unit cell dimensions	a = 12.5935(3) Å	≤ 90°.
	b = 12.7118(6) Å	ℳ = 93.663(2)°.
	c = 19.2504(4) Å	ℳ = 90°.
Volume	3075.43(17) Å <sup>3</sup>	
Z	4	
Density (calculated)	1.623 Mg/m <sup>3</sup>	
Absorption coefficient	0.803 mm <sup>-1</sup>	
F(000)	1540	
Crystal size	0.08 x 0.06 x 0.06 mm <sup>3</sup>	
Theta range for data collection	3.38 to 27.49°.	
Index ranges	-16<=h<=16, -11<=k<=16, -24<=l<=24	
Reflections collected	9892	
Independent reflections	6977 [R(int) = 0.0203]	
Completeness to theta = 27.49°	98.8 %	
Absorption correction	Semi-empirical from equivalents	
Max. and min. transmission	0.9534 and 0.9386	
Refinement method	Full-matrix least-squares on F <sup>2</sup>	
Data / restraints / parameters	6977 / 0 / 465	
Goodness-of-fit on F <sup>2</sup>	1.080	
Final R indices [I>2sigma(I)]	R1 = 0.0446, wR2 = 0.0896	
R indices (all data)	R1 = 0.0565, wR2 = 0.0995	
Largest diff. peak and hole	0.553 and -0.401 e.Å <sup>-3</sup>	

**Table S2.** Atomic coordinates ( $\times 10^4$ ) and equivalent isotropic displacement parameters ( $\text{\AA}^2 \times 10^3$ ) for 1.  $U(\text{eq})$  is defined as one third of the trace of the orthogonalized  $U^{ij}$  tensor.

	<i>x</i>	<i>y</i>	<i>z</i>	$U(\text{eq})$
Co(1)	2497(1)	2193(1)	9810(1)	20(1)
Cl(1)	1341(1)	5748(1)	8719(1)	30(1)
Cl(2)	3705(1)	5519(1)	11260(1)	33(1)
O(2)	1169(2)	184(1)	8000(1)	27(1)
N(4)	4026(2)	2083(2)	10339(1)	23(1)
O(1)	2481(2)	3781(2)	9903(1)	30(1)
O(3)	3710(2)	-252(1)	11414(1)	28(1)
N(5)	1989(2)	1896(2)	10871(1)	21(1)
N(3)	2520(2)	555(2)	9718(1)	21(1)
N(2)	2959(2)	2209(2)	8763(1)	22(1)
N(1)	941(2)	2235(2)	9260(1)	23(1)
C(14)	2511(2)	1514(2)	8301(1)	21(1)
C(13)	2785(2)	1485(2)	7616(1)	24(1)
C(16)	-245(2)	1596(2)	8325(1)	26(1)
C(20)	1203(2)	2438(2)	11140(1)	25(1)
O(10)	2788(2)	4832(2)	11131(1)	39(1)
C(25)	4211(2)	1328(2)	10819(1)	22(1)
C(23)	2044(2)	777(2)	11881(1)	26(1)
C(19)	218(2)	2983(2)	9381(1)	26(1)
C(4)	2488(2)	-1076(2)	10325(1)	28(1)
C(22)	1207(2)	1340(2)	12140(1)	29(1)
C(18)	-744(2)	3076(2)	8996(1)	30(1)
C(5)	2802(2)	-32(2)	10279(1)	22(1)
C(1)	1919(2)	125(2)	9185(1)	22(1)
C(3)	1843(2)	-1503(2)	9793(1)	32(1)
C(15)	711(2)	1566(2)	8725(1)	22(1)
C(21)	790(2)	2186(2)	11769(1)	27(1)
C(29)	4746(2)	2855(2)	10290(1)	28(1)
C(17)	-982(2)	2358(2)	8471(1)	29(1)
C(6)	1609(2)	814(2)	8549(1)	22(1)
C(2)	1539(2)	-896(2)	9222(1)	29(1)
C(7)	3335(2)	513(2)	10924(1)	22(1)
C(12)	3556(2)	2168(2)	7403(1)	27(1)

C(24)	2415(2)	1088(2)	11250(1)	21(1)
C(11)	4001(2)	2892(2)	7866(1)	28(1)
C(10)	3671(2)	2897(2)	8539(1)	24(1)
O(5)	378(2)	5420(2)	8355(1)	56(1)
O(6)	2113(2)	4913(2)	8698(1)	52(1)
C(9)	4549(3)	-935(2)	11202(2)	38(1)
O(9)	4431(2)	5359(2)	10741(2)	71(1)
O(4)	1730(2)	6669(2)	8393(2)	57(1)
C(26)	5127(2)	1352(2)	11272(1)	28(1)
C(28)	5675(2)	2912(2)	10713(2)	35(1)
C(8)	1808(3)	-628(2)	7720(2)	33(1)
O(7)	1152(2)	5969(2)	9426(1)	60(1)
C(27)	5860(2)	2153(2)	11215(2)	33(1)
O(11)	4212(2)	5237(3)	11919(2)	76(1)
O(8)	3372(2)	6568(2)	11274(2)	83(1)

---

**Table S3.** Bond lengths [ $\text{\AA}$ ] and angles [ $^\circ$ ] for **1**.

Co(1)-O(1)	2.027(2)
Co(1)-N(3)	2.090(2)
Co(1)-N(4)	2.124(2)
Co(1)-N(2)	2.134(2)
Co(1)-N(1)	2.168(2)
Co(1)-N(5)	2.211(2)
Cl(1)-O(5)	1.423(2)
Cl(1)-O(7)	1.424(2)
Cl(1)-O(4)	1.429(2)
Cl(1)-O(6)	1.442(2)
Cl(2)-O(8)	1.399(3)
Cl(2)-O(9)	1.411(3)
Cl(2)-O(11)	1.428(3)
Cl(2)-O(10)	1.456(2)
O(2)-C(6)	1.412(3)
O(2)-C(8)	1.435(3)
N(4)-C(25)	1.342(3)
N(4)-C(29)	1.344(3)
O(1)-H(1B)	0.84(4)
O(1)-H(1A)	0.79(4)
O(3)-C(7)	1.414(3)
O(3)-C(9)	1.446(3)
N(5)-C(20)	1.337(3)
N(5)-C(24)	1.351(3)
N(3)-C(5)	1.342(3)
N(3)-C(1)	1.349(3)
N(2)-C(10)	1.343(3)
N(2)-C(14)	1.352(3)
N(1)-C(19)	1.346(3)
N(1)-C(15)	1.353(3)
C(14)-C(13)	1.385(3)
C(14)-C(6)	1.543(3)
C(13)-C(12)	1.383(4)
C(13)-H(13)	0.9500
C(16)-C(17)	1.383(4)
C(16)-C(15)	1.387(3)

C(16)-H(16)	0.9500
C(20)-C(21)	1.384(4)
C(20)-H(20)	0.9500
C(25)-C(26)	1.402(3)
C(25)-C(7)	1.536(3)
C(23)-C(24)	1.386(3)
C(23)-C(22)	1.393(4)
C(23)-H(23)	0.9500
C(19)-C(18)	1.384(4)
C(19)-H(19)	0.9500
C(4)-C(3)	1.378(4)
C(4)-C(5)	1.389(4)
C(4)-H(4)	0.9500
C(22)-C(21)	1.377(4)
C(22)-H(22)	0.9500
C(18)-C(17)	1.382(4)
C(18)-H(18)	0.9500
C(5)-C(7)	1.538(3)
C(1)-C(2)	1.387(4)
C(1)-C(6)	1.536(3)
C(3)-C(2)	1.377(4)
C(3)-H(3)	0.9500
C(15)-C(6)	1.535(3)
C(21)-H(21)	0.9500
C(29)-C(28)	1.385(4)
C(29)-H(29)	0.9500
C(17)-H(17)	0.9500
C(2)-H(2)	0.9500
C(7)-C(24)	1.538(3)
C(12)-C(11)	1.375(4)
C(12)-H(12)	0.9500
C(11)-C(10)	1.388(4)
C(11)-H(11)	0.9500
C(10)-H(10)	0.9500
C(9)-H(9C)	0.97(4)
C(9)-H(9A)	0.99(4)
C(9)-H(9B)	0.91(4)
C(26)-C(27)	1.383(4)

C(26)-H(26)	0.9500
C(28)-C(27)	1.375(4)
C(28)-H(28)	0.9500
C(8)-H(8A)	0.98(3)
C(8)-H(8B)	0.95(3)
C(8)-H(8C)	1.00(3)
C(27)-H(27)	0.9500
O(1)-Co(1)-N(3)	179.73(9)
O(1)-Co(1)-N(4)	92.13(8)
N(3)-Co(1)-N(4)	87.61(8)
O(1)-Co(1)-N(2)	94.50(9)
N(3)-Co(1)-N(2)	85.58(8)
N(4)-Co(1)-N(2)	99.17(8)
O(1)-Co(1)-N(1)	90.26(8)
N(3)-Co(1)-N(1)	90.00(8)
N(4)-Co(1)-N(1)	177.58(8)
N(2)-Co(1)-N(1)	80.26(8)
O(1)-Co(1)-N(5)	94.79(8)
N(3)-Co(1)-N(5)	85.14(8)
N(4)-Co(1)-N(5)	81.56(8)
N(2)-Co(1)-N(5)	170.65(8)
N(1)-Co(1)-N(5)	98.62(8)
O(5)-Cl(1)-O(7)	109.83(18)
O(5)-Cl(1)-O(4)	109.18(15)
O(7)-Cl(1)-O(4)	110.00(17)
O(5)-Cl(1)-O(6)	108.93(16)
O(7)-Cl(1)-O(6)	109.03(15)
O(4)-Cl(1)-O(6)	109.85(16)
O(8)-Cl(2)-O(9)	111.1(2)
O(8)-Cl(2)-O(11)	109.9(2)
O(9)-Cl(2)-O(11)	108.6(2)
O(8)-Cl(2)-O(10)	109.79(16)
O(9)-Cl(2)-O(10)	109.59(15)
O(11)-Cl(2)-O(10)	107.84(15)
C(6)-O(2)-C(8)	119.1(2)
C(25)-N(4)-C(29)	118.9(2)
C(25)-N(4)-Co(1)	119.28(17)

C(29)-N(4)-Co(1)	120.86(17)
Co(1)-O(1)-H(1B)	120(3)
Co(1)-O(1)-H(1A)	123(3)
H(1B)-O(1)-H(1A)	116(4)
C(7)-O(3)-C(9)	116.3(2)
C(20)-N(5)-C(24)	117.4(2)
C(20)-N(5)-Co(1)	122.34(16)
C(24)-N(5)-Co(1)	120.03(16)
C(5)-N(3)-C(1)	119.5(2)
C(5)-N(3)-Co(1)	119.30(16)
C(1)-N(3)-Co(1)	117.24(16)
C(10)-N(2)-C(14)	118.3(2)
C(10)-N(2)-Co(1)	122.51(17)
C(14)-N(2)-Co(1)	119.22(17)
C(19)-N(1)-C(15)	117.4(2)
C(19)-N(1)-Co(1)	122.24(17)
C(15)-N(1)-Co(1)	119.95(17)
N(2)-C(14)-C(13)	121.7(2)
N(2)-C(14)-C(6)	117.2(2)
C(13)-C(14)-C(6)	120.9(2)
C(12)-C(13)-C(14)	119.2(2)
C(12)-C(13)-H(13)	120.4
C(14)-C(13)-H(13)	120.4
C(17)-C(16)-C(15)	118.4(2)
C(17)-C(16)-H(16)	120.8
C(15)-C(16)-H(16)	120.8
N(5)-C(20)-C(21)	123.2(2)
N(5)-C(20)-H(20)	118.4
C(21)-C(20)-H(20)	118.4
N(4)-C(25)-C(26)	120.9(2)
N(4)-C(25)-C(7)	118.6(2)
C(26)-C(25)-C(7)	120.1(2)
C(24)-C(23)-C(22)	118.2(2)
C(24)-C(23)-H(23)	120.9
C(22)-C(23)-H(23)	120.9
N(1)-C(19)-C(18)	123.1(2)
N(1)-C(19)-H(19)	118.4
C(18)-C(19)-H(19)	118.4

C(3)-C(4)-C(5)	119.0(2)
C(3)-C(4)-H(4)	120.5
C(5)-C(4)-H(4)	120.5
C(21)-C(22)-C(23)	119.2(2)
C(21)-C(22)-H(22)	120.4
C(23)-C(22)-H(22)	120.4
C(17)-C(18)-C(19)	118.5(3)
C(17)-C(18)-H(18)	120.8
C(19)-C(18)-H(18)	120.8
N(3)-C(5)-C(4)	121.4(2)
N(3)-C(5)-C(7)	118.6(2)
C(4)-C(5)-C(7)	119.3(2)
N(3)-C(1)-C(2)	121.3(2)
N(3)-C(1)-C(6)	118.4(2)
C(2)-C(1)-C(6)	120.2(2)
C(2)-C(3)-C(4)	119.6(3)
C(2)-C(3)-H(3)	120.2
C(4)-C(3)-H(3)	120.2
N(1)-C(15)-C(16)	122.8(2)
N(1)-C(15)-C(6)	115.7(2)
C(16)-C(15)-C(6)	121.3(2)
C(22)-C(21)-C(20)	118.8(2)
C(22)-C(21)-H(21)	120.6
C(20)-C(21)-H(21)	120.6
N(4)-C(29)-C(28)	123.0(3)
N(4)-C(29)-H(29)	118.5
C(28)-C(29)-H(29)	118.5
C(18)-C(17)-C(16)	119.7(2)
C(18)-C(17)-H(17)	120.2
C(16)-C(17)-H(17)	120.2
O(2)-C(6)-C(15)	105.04(19)
O(2)-C(6)-C(1)	109.9(2)
C(15)-C(6)-C(1)	109.4(2)
O(2)-C(6)-C(14)	110.9(2)
C(15)-C(6)-C(14)	106.1(2)
C(1)-C(6)-C(14)	114.9(2)
C(3)-C(2)-C(1)	119.0(2)
C(3)-C(2)-H(2)	120.5

C(1)-C(2)-H(2)	120.5
O(3)-C(7)-C(25)	109.8(2)
O(3)-C(7)-C(24)	106.38(19)
C(25)-C(7)-C(24)	107.5(2)
O(3)-C(7)-C(5)	109.8(2)
C(25)-C(7)-C(5)	118.5(2)
C(24)-C(7)-C(5)	104.02(19)
C(11)-C(12)-C(13)	119.5(2)
C(11)-C(12)-H(12)	120.2
C(13)-C(12)-H(12)	120.2
N(5)-C(24)-C(23)	123.1(2)
N(5)-C(24)-C(7)	115.1(2)
C(23)-C(24)-C(7)	121.8(2)
C(12)-C(11)-C(10)	118.3(2)
C(12)-C(11)-H(11)	120.8
C(10)-C(11)-H(11)	120.8
N(2)-C(10)-C(11)	122.9(2)
N(2)-C(10)-H(10)	118.6
C(11)-C(10)-H(10)	118.6
O(3)-C(9)-H(9C)	105(2)
O(3)-C(9)-H(9A)	110(2)
H(9C)-C(9)-H(9A)	112(3)
O(3)-C(9)-H(9B)	107(3)
H(9C)-C(9)-H(9B)	111(3)
H(9A)-C(9)-H(9B)	111(3)
C(27)-C(26)-C(25)	119.5(3)
C(27)-C(26)-H(26)	120.2
C(25)-C(26)-H(26)	120.2
C(27)-C(28)-C(29)	118.4(3)
C(27)-C(28)-H(28)	120.8
C(29)-C(28)-H(28)	120.8
O(2)-C(8)-H(8A)	105.8(17)
O(2)-C(8)-H(8B)	107.9(18)
H(8A)-C(8)-H(8B)	112(2)
O(2)-C(8)-H(8C)	112.8(19)
H(8A)-C(8)-H(8C)	110(2)
H(8B)-C(8)-H(8C)	109(3)
C(28)-C(27)-C(26)	119.3(3)

C(28)-C(27)-H(27)	120.4
C(26)-C(27)-H(27)	120.4

Symmetry transformations used to generate equivalent atoms:

**Table S4** Anisotropic displacement parameters ( $\text{\AA}^2 \times 10^3$ ) for **1**. The anisotropic displacement factor exponent takes the form:  $-2\Box^2 [ h^2 a^{*2} U^{11} + \dots + 2 h k a^{*} b^{*} U^{12} ]$

	U <sup>11</sup>	U <sup>22</sup>	U <sup>33</sup>	U <sup>23</sup>	U <sup>13</sup>	U <sup>12</sup>
Co(1)	22(1)	18(1)	20(1)	0(1)	0(1)	0(1)
Cl(1)	35(1)	24(1)	30(1)	0(1)	-3(1)	5(1)
Cl(2)	31(1)	31(1)	38(1)	-3(1)	6(1)	-9(1)
O(2)	30(1)	26(1)	25(1)	-7(1)	-2(1)	-3(1)
N(4)	23(1)	22(1)	24(1)	0(1)	1(1)	0(1)
O(1)	44(1)	21(1)	25(1)	1(1)	-7(1)	1(1)
O(3)	30(1)	25(1)	28(1)	6(1)	0(1)	7(1)
N(5)	21(1)	22(1)	20(1)	0(1)	1(1)	0(1)
N(3)	21(1)	20(1)	21(1)	-1(1)	2(1)	1(1)
N(2)	22(1)	23(1)	21(1)	0(1)	1(1)	1(1)
N(1)	22(1)	25(1)	21(1)	2(1)	2(1)	1(1)
C(14)	20(1)	19(1)	23(1)	1(1)	2(1)	3(1)
C(13)	29(1)	21(1)	23(1)	0(1)	0(1)	2(1)
C(16)	24(1)	29(1)	24(1)	3(1)	-1(1)	-5(1)
C(20)	25(1)	27(1)	22(1)	-1(1)	0(1)	4(1)
O(10)	41(1)	46(1)	31(1)	-6(1)	7(1)	-21(1)
C(25)	22(1)	22(1)	24(1)	-1(1)	3(1)	5(1)
C(23)	28(1)	25(1)	26(1)	2(1)	1(1)	-3(1)
C(19)	28(1)	27(1)	23(1)	0(1)	3(1)	1(1)
C(4)	37(2)	21(1)	27(1)	1(1)	3(1)	-2(1)
C(22)	29(1)	32(1)	25(1)	1(1)	4(1)	-4(1)
C(18)	27(1)	34(2)	29(1)	4(1)	5(1)	4(1)
C(5)	22(1)	21(1)	24(1)	1(1)	4(1)	1(1)
C(1)	21(1)	23(1)	21(1)	-1(1)	4(1)	0(1)
C(3)	45(2)	21(1)	31(1)	-3(1)	7(1)	-9(1)
C(15)	22(1)	26(1)	20(1)	1(1)	3(1)	-2(1)
C(21)	24(1)	32(1)	27(1)	-5(1)	3(1)	2(1)
C(29)	27(1)	28(1)	30(1)	2(1)	1(1)	-5(1)

C(17)	21(1)	37(2)	28(1)	9(1)	0(1)	0(1)
C(6)	23(1)	22(1)	21(1)	-2(1)	-1(1)	-3(1)
C(2)	37(2)	26(1)	24(1)	-3(1)	3(1)	-8(1)
C(7)	24(1)	20(1)	22(1)	4(1)	0(1)	3(1)
C(12)	30(1)	28(1)	24(1)	5(1)	4(1)	3(1)
C(24)	21(1)	21(1)	22(1)	-2(1)	-2(1)	-1(1)
C(11)	25(1)	28(1)	30(1)	7(1)	3(1)	-1(1)
C(10)	24(1)	24(1)	25(1)	3(1)	-1(1)	-1(1)
O(5)	54(2)	45(1)	66(2)	0(1)	-23(1)	-7(1)
O(6)	67(2)	48(1)	43(1)	11(1)	11(1)	30(1)
C(9)	34(2)	25(2)	53(2)	3(1)	-3(1)	12(1)
O(9)	69(2)	64(2)	86(2)	-15(2)	50(2)	-22(2)
O(4)	47(2)	41(1)	81(2)	25(1)	-2(1)	-2(1)
C(26)	26(1)	27(1)	30(1)	0(1)	-1(1)	7(1)
C(28)	26(1)	35(2)	42(2)	1(1)	-1(1)	-7(1)
C(8)	48(2)	25(1)	26(1)	-6(1)	6(1)	-1(1)
O(7)	86(2)	56(2)	38(1)	-14(1)	6(1)	14(2)
C(27)	23(1)	36(2)	40(2)	0(1)	-7(1)	0(1)
O(11)	71(2)	93(2)	60(2)	22(2)	-21(1)	-43(2)
O(8)	50(2)	32(1)	167(3)	-14(2)	-1(2)	2(1)

---

**Table S5.** Hydrogen bonds for **1** ( $\text{\AA}$  and  $^\circ$ ).

D-H...A	d(D-H)	d(H...A)	d(D...A)	$\angle$ (DHA)
O(1)-H(1B)...O(6)	0.84(4)	1.92(4)	2.744(3)	170(4)
O(1)-H(1A)...O(10)	0.79(4)	1.93(4)	2.721(3)	174(4)

Symmetry transformations used to generate equivalent atoms:

**Table S6.** Density functional theory optimized geometry coordinates of  $[\text{Co}^{\text{IV}}(\text{Py5-OH})(\text{OH})]^{2+}$  at a B3LYP/Lanl2DZ level of theory. Note the methyl groups of the methoxy have been replaced by hydroxide groups to facilitate more rapid calculation time.

Standard orientation:

Center	Atomic	Atomic	Coordinates (Angstroms)		
Number	Number	Type	X	Y	Z
<hr/>					
1	8	0	-3.484033	0.028282	2.163202
2	8	0	3.747819	-0.037481	1.802470
3	7	0	0.088242	-0.002172	1.286155
4	7	0	-1.530045	-1.317769	-0.677534
5	7	0	-1.587785	1.275466	-0.667767
6	7	0	1.443117	1.423401	-0.695684
7	7	0	1.507391	-1.360686	-0.726229
8	6	0	-1.047987	-0.002948	2.037176
9	6	0	-1.005747	0.033631	3.436641
10	6	0	0.239894	-0.004033	4.083269
11	6	0	1.408943	-0.040453	3.303286
12	6	0	1.303862	-0.001528	1.908298
13	6	0	-2.368842	-0.032013	1.277920

14	6	0	-2.449384	-1.254641	0.330148
15	6	0	-3.522617	-2.152597	0.384697
16	6	0	-3.671040	-3.122837	-0.625443
17	6	0	-2.775927	-3.111392	-1.708329
18	6	0	-1.726796	-2.183768	-1.711749
19	6	0	-2.483625	1.198105	0.359118
20	6	0	-3.547984	2.099335	0.477192
21	6	0	-3.730378	3.074965	-0.521988
22	6	0	-2.879110	3.066076	-1.641886
23	6	0	-1.822191	2.148187	-1.689463
24	6	0	2.555298	0.023061	1.022835
25	6	0	2.536682	1.257972	0.102979
26	6	0	3.621094	2.145521	0.053649
27	6	0	3.573316	3.255790	-0.808812
28	6	0	2.435264	3.432576	-1.615205
29	6	0	1.398610	2.495017	-1.542199
30	6	0	2.560439	-1.221762	0.130818
31	6	0	3.616400	-2.141342	0.174912
32	6	0	3.604152	-3.240228	-0.702803

33	6	0	2.536238	-3.367343	-1.609988
34	6	0	1.509708	-2.415717	-1.595712
35	1	0	-1.923119	0.101567	4.008114
36	1	0	0.300145	-0.005093	5.167668
37	1	0	2.381838	-0.110978	3.773557
38	1	0	-4.268205	-2.070527	1.166553
39	1	0	-4.495497	-3.828868	-0.592580
40	1	0	-2.895491	-3.783467	-2.551679
41	1	0	-1.089399	-2.085589	-2.576899
42	1	0	-1.209586	2.059552	-2.574710
43	1	0	-3.033746	3.740888	-2.477454
44	1	0	-4.547007	3.787361	-0.451433
45	1	0	-4.228136	2.000835	1.314210
46	1	0	4.503489	1.959304	0.654280
47	1	0	4.404743	3.952763	-0.857527
48	1	0	2.350252	4.267269	-2.303196
49	1	0	0.531952	2.609918	-2.171216
50	1	0	4.422254	-1.977796	0.879361
51	1	0	4.410570	-3.967403	-0.687475

52	1	0	2.492073	-4.183350	-2.323843
53	1	0	0.692231	-2.504894	-2.291724
54	8	0	-0.060353	0.017734	-2.477859
55	1	0	-3.570382	-0.743839	2.763001
56	1	0	3.894653	0.742999	2.379602
57	27	0	-0.008220	0.006654	-0.692484
58	1	0	0.814759	0.037903	-2.940824

---

## References

1. R. T. Jonas and T. D. P. Stack, *J. Am. Chem. Soc.*, 1997, **119**, 8566-8567.